(3) E. Secher-Hansen, H. Langgard, and J. Schou, *Acta Pharmacol. Toxicol.*, **25**, 162, 290 (1967).
(4) *Ibid.*, **26**, 9 (1968).
(5) B. E. Ballard and E. Menczel, *J. Pharm. Sci.*, **56**, 1476 (1967).
(6) R. H. Levy and M. Rowland, *J. Pharmacokinet. Biopharm.*, **2**, 313, 337 (1974).
(7) R. B. Sund and J. Shou, *Acta Pharmacol. Toxicol.*, **21**, 313 (1964).
(8) M. Pfeffer and D. R. Van Harken, *J. Pharm. Sci.*, **70**, 449 (1981).
(9) T. Tanaka, H. Kobayashi, K. Okumura, S. Muranishi, and H. Sezaki, *Chem. Pharm. Bull.*, **22**, 175 (1974).
(10) J. H. Leathem, *Proc. Soc. Exp. Biol. Med.*, **68**, 92 (1948).
(11) W. L. Honrath, A. Wolff, and A. Meli, *Steroids*, **2**, 425 (1963).
(12) J. J. Nora, W. D. Smith, and J. R. Cameron, *J. Pediatr.*, **64**, 547 (1964).
(13) E. A. Brown, T. G. Metcalf, and L. W. Slanety, *Ann. Allergy*, **19**, 1016 (1961).
(14) R. Deanesly and A. S. Parkes, *J. Physiol.*, **78**, 155 (1933).
(15) J. C. Bauernfeind and H. L. Newmark, *Bull. Parenter. Drug Assoc.*, **24**, 169 (1970).
(16) S. Muranishi, *Yakugaku Zasshi*, **100**, 687 (1980).
(17) C. L. J. Coles, K. R. Heath, M. L. Hilton, K. A. Lees, P. W. Muggleton, and C. A. Walton, *J. Pharm. Pharmacol.*, **17**, 87S (1965).

ACKNOWLEDGMENTS

The authors thank Mrs. J. Kagawa for her technical assistance and thank Prof. M. Nakagaki, Kyoto University, for his valuable comments on the manuscript.

Studies on the Absorption of Practically Water-Insoluble Drugs Following Injection VI: Subcutaneous Absorption from Aqueous Suspensions in Rats

KOICHIRO HIRANO ˣ and HIDEO YAMADA

Received April 8, 1981, from the *Shionogi Research Laboratories, Shionogi & Co., Ltd., Fukushima-ku, Osaka, 553, Japan.* Accepted for publication May 20, 1981.

Abstract □ The absorption characteristics and kinetics of practically water-insoluble drugs following subcutaneous injection of their aqueous suspensions were investigated in intact rats by the local clearance method and compared with those following intramuscular injection reported previously. The plot of the cube root of the residual fraction of the drug in the injection site *versus* time gave a good linear relationship under various experimental conditions. The absorption rate constant (j) increased with decreasing particle size. This increase was remarkable in the region of mean particle diameter <2–3 μm, while it was gradual or slight in the region above this. This phenomenon was explained by the fact that the *in vivo* spreading of particles of more than ~3 μm was still more limited by the network of the fibrous tissues. Between j and the initial drug concentration (C_0) or injection volume (V_0), the practically important relationship $j \propto C_0^g V_0^h$ ($g = -0.66$ and $h = -0.32$) could approximately be derived from the experimental results. Comparison of j values among various compounds with different solubility (C_s') in saline but with similar colloidal properties (particle size distribution and sedimentation volume) showed that a log j *versus* log C_s' plot gave a nearly straight line with a slope of ~0.5. All the results observed for the subcutaneous absorption were similar to those for intramuscular absorption and could reasonably be explained by the kinetic model proposed for intramuscular absorption.

Keyphrases □ Absorption, subcutaneous—from aqueous suspensions of practically water-insoluble drugs, rats □ Water-insoluble drugs—subcutaneous absorption from aqueous suspensions, rats □ Aqueous suspensions—subcutaneous absorption of practically water-insoluble drugs, rats

Although subcutaneous administration of aqueous suspensions is very popular for practically water-insoluble drugs in preclinical animal experiments, little has been studied on their absorption mechanisms and kinetics except for the particle-size effect on pharmacological responses (1). Previously investigated (2, 3) were the absorption behaviors of subcutaneously implanted solid drugs (sphere, disk, and cylindrical shapes) and the absorption kinetic process was clarified. The intramuscular absorption characteristics of practically water-insoluble drugs from aqueous suspension were investigated in detail, and a kinetic equation was proposed for the drug absorption, which was obtained empirically and was very useful (4).

In the present work, similar investigations for the subcutaneous route were done with the local clearance method in intact rats. The purpose of the present study was to clarify the relationship between the absorption rate and physicochemical properties (particle size, initial drug concentration, injection volume, drug solubility, *etc.*), to express this relationship in appropriate mathematical terms, and to compare the results with those for the intramuscular route reported previously (4).

The findings obtained in this study will offer a novel and useful guide for more detailed screening and preclinical testing in laboratory animals of new drugs under development.

EXPERIMENTAL

Materials—Azo dyes (*p*-aminoazobenzene, *p*-hydroxyazobenzene, *o*-aminoazotoluene, and 1-phenylazo-2-naphthylamine), sulfa drugs (N^1-acetylsulfamethoxazole and sulfamethoxazole), and a steroid (betamethasone dipropionate[1]) were used as models for practically water-insoluble drugs. These azo dyes and sulfa drugs were the same as those used in a previous study (4). Betamethasone dipropionate was of medicinal grade and its purity was ascertained to be satisfactory through elementary analysis, melting point measurement, and TLC. Methylcellulose[2] and polysorbate 80[3], used as dispersing agents for preparations, were the same as those reported previously (4). All other chemicals were of analytical or reagent grade.

To compare the spreading area of injected particles, the following standard particles of different sizes were also used: two polystyrene latexes (0.721 and 1.305 μm in mean diameter based on number size distribution)[4], polyvinyltoluene latex (2.956 μm)[4], spores (4.94 μm)[5], di-

[1] Schering Corp., Bloomfield, N.J.
[2] Metolose SM-15, Shinetsu Kagaku Kogyo Co., Ltd., Tokyo.
[3] Kao Atlas Co., Ltd., Tokyo.
[4] The Dow Chemical Co., Indianapolis, Ind.
[5] Coulter Electronics, Ltd., Dunstable.

0022-3549/82/0500-0500$01.00/0

Table I—Particle Size (D_{ss}), Distribution Constant (n), and Sedimentation Volume (V_{sed}) of Aqueous Suspensions of Test Compounds Prepared by the Controlled Preparation Method

Compound	D_{ss}, μm[a]	n[b]	V_{sed}, cm³/g
Sulfamethoxazole	4.0	2.9	1.7
N^1-Acetylsulfamethoxazole	3.5	2.6	1.7
p-Aminoazobenzene	4.2	2.7	2.0
p-Hydroxyazobenzene	3.6–4.1	2.5–2.7	2.8–3.1
o-Aminoazotoluene	3.9	2.7	2.4
1-Phenylazo-2-naphthylamine	4.0	2.5	2.2

[a] Mean particle diameter obtained from Rosin-Rammler plot. [b] This value (obtained from Rosin-Rammler plot) shows the degree of narrowness of particle size distribution. The larger the value, the narrower the particle size distribution.

vinylbenzene latex (8.99 μm)[4], and ragweed pollen (17.95 μm)[5]. These are nearly spherical and commonly used as size calibrators for particle size measurements.

Preparation of Test Suspensions—Unless otherwise mentioned, the vehicle composed of 0.5% (w/v) of methylcellulose, 0.005% of polysorbate 80, and 0.9% NaCl was used as a dispersion medium for the same reason mentioned previously (4). This vehicle was presaturated with the drug to be dispersed and filtered through a membrane filter[6], then used for making the various preparations. To regulate particle size, all test aqueous suspensions were prepared by fractionation techniques using natural or centrifugal sedimentation. The suspensions formulated according to the controlled preparation method in which they were intended to contain particles of ~4 μm in average diameter, described in the previous report (4), were used unless otherwise mentioned. Hereafter, these suspensions are referred to as controlled suspensions. Colloidal properties such as mean particle diameters (D_{ss}), distribution constants (n), and sedimentation volumes (V_{sed}) of the test suspensions prepared by this method appear in Table I. The suspensions other than the controlled ones were prepared by similar methods with appropriate modifications. After adjustment of the drug concentration in a test suspension, it was stored at 25° until use. The syringeability for all the suspensions was good in the same needle (25G × 2.54 cm)[7] and syringe used in the absorption experiment.

Procedure of Absorption Experiment—Male Wistar albino rats (250–290 g) were used in all absorption experiments. The subcutaneous region near the center of the dorsum of intact rat was selected as a model injection site and the same local clearance method described in the previous paper (5) was employed for the present investigations. Since almost all of the drug remaining in the injection site was undissolved and unchanged, the absorption experiment adopted was considered to be appropriate for understanding the true absorption phenomena from the systems of interest.

Measurement of Physicochemical Properties of Test Compounds and Suspensions—For the solubilities of model drugs in 0.9% (w/v) NaCl (saline) or in pH 7.25 phosphate buffer (0.067 *M* Na_2HPO_4–KH_2PO_4) isotonized with NaCl, previously obtained data (4) were used. The solubilities in 2% (w/v) bovine serum albumin[8] in pH 7.25 isotonic phosphate buffer were determined according to a method similar to that described in the previous paper (4). The density (ρ) of the model compound, and the sedimentation volume (V_{sed}) and particle size distribution (D_{ss} and n) of each test suspension were also measured by the methods described in the previous report (4).

Analytical Method—*Samples from Absorption Experiments*—The amounts of test compounds other than betamethasone dipropionate remaining in the injection site were determined colorimetrically as described previously (4). Betamethasone dipropionate was analyzed by the HPLC method under the following conditions: HPLC apparatus[9]; UV detector (254 nm); column[10], 25 cm × 2.1-mm ϕ; mobile phase, *n*-hexane–isopropyl ether–ethanol–H_2O (5:20:1.5:10, v/v, upper layer); flow rate (pressure), 0.43–0.46 ml/min (84 kg/cm²).

Samples from Other Experiments—The concentrations of model compounds other than betamethasone dipropionate in test suspensions were analyzed spectrophotometrically as described in the previous paper (4). For the analysis of betamethasone dipropionate, the optical density was read at 243 nm after dilution with ethanol–H_2O (1:1, v/v). The sample solutions (filtrate or supernate) for the determination of the solubilities of azo compounds in 2% bovine serum albumin solution were assayed by a colorimetric method similar to that reported previously (4). Those of sulfa drugs were assayed as follows: One milliliter of the sample solution was thoroughly mixed with 5 ml of pH 4.7 buffer [1 *N* HCl–1 *N* CH_3COONa, 3:7 (v/v)] and from this mixture the sulfa drug was extracted with 10 ml of ethyl acetate. A portion of this extract was freed of the solvent *in vacuo* then assayed colorimetrically after diazotization according to the method described in the previous paper (4).

[6] Millipore membrane filter HA., Millipore Corp., Bedford, Mass.
[7] Terumo Co., Ltd., Tokyo.
[8] Sigma Chemical Co., St. Louis, Mo.
[9] Dupont 830 LC,
[10] Zorbax SIL,

Table II—List of Data (C_0, V_0, and j for *p*-Hydroxyazobenzene Suspension[a]) Used for Estimation of Parameters g and h, and the Values Estimated[b]

C_0, mg/ml	V_0, ml	j, hr^{-1}	Comment
0.5	0.50	0.27	V_0: constant
1.0	0.50	0.14	
20.0	0.50	0.025	
50.0	0.50	0.015	
5.0	0.05	0.12	C_0: constant
5.0	0.10	0.10	
5.0	0.50	0.046	
5.0	2.00	0.032	
50.0	0.050	0.020	W_0: constant
25.0	0.10	0.027	
2.5	1.00	0.045	
1.25	2.00	0.11	

$g = -0.656$ (0.049), $h = -0.315$ (0.057)

[a] Controlled suspension. [b] The values g and h were estimated by multiple regression analysis and are given together with the standard errors in parentheses.

RESULTS AND DISCUSSION

State of the Depot and Drug Absorption Kinetics—Although the subcutaneous region is composed of networks of loosely cross-linked fibrous tissues, injected solutions form a pool (depot) with lateral spread (6, 7). This was also observed in experiments using aqueous suspensions of some dyes and uniform latexes. In addition, the suspension particles were confined to such networks and their spreading was not so extensive as that of the aqueous dispersion medium (vehicle) after injection. For example, even in the case of a 1-ml injection of 0.5% (w/v) of uniform latex of 0.7 μm in diameter (this size seems to be the approximate lower limit for common preparations) into the dorsal subcutaneous region of rats, the resulting lateral spreading area of the particles did not exceed ~30% of that of the aqueous vehicle. This spreading area became smaller with increasing particle size. These findings clearly indicated that the subcutaneously injected particles were loosely agglomerated at the injection site.

In common cases, a drug in aqueous suspension injected subcutaneously must first become dissolved in the tissue fluids surrounding the particle agglomerate, diffuse into the intercellular space (or intracellular region) of the connective tissues, and then permeate the vascular membranes until it enters the blood or lymph stream. The participation of direct absorption of the fine particles by phagocytosis or some other mechanisms can not be completely denied (8, 9). However, their contribution to the drug absorption may be much smaller than that of the above mentioned mechanism *via* the dissolution process except for exceedingly fine particles of water-insoluble drugs (10).

It was indicated previously (11) that the connective tissue ground substance formed a diffusion barrier to the subcutaneous absorption of carbohydrates with different molecular weights in aqueous solution. The relationship between the absorption rates of a variety of compounds subcutaneously implanted in rats and their physicochemical properties

Table III—Check of Experimentally Determined g and h Values Using Betamethasone Dipropionate Aqueous Suspensions

Experiment Number	C_0, mg/ml	V_0, ml	$j(i)/j(1)$ Calculated	$j(i)/j(1)$ Experimental
1[a]	2	0.05		
	2	0.50	0.48	0.49 (0.03)
2[b]	1	0.50		
	10	0.50	0.22	0.26 (0.03)

[a] Vehicle, 0.01% (w/v) polysorbate 80 + 0.01% (w/v) benzalkonium chloride + 0.38% (w/v) $NaH_2PO_4 \cdot 2H_2O$ + 1.79% (w/v) $Na_2HPO_4 \cdot 12H_2O$; D_{ss} (n), 7.1 μm (2.5). [b] Vehicle, 0.5% (w/v) methylcellulose SM-15 + 0.01% (w/v) polysorbate 80 + 0.9% (w/v) NaCl; D_{ss} (n), 2.5 μm (2.6).

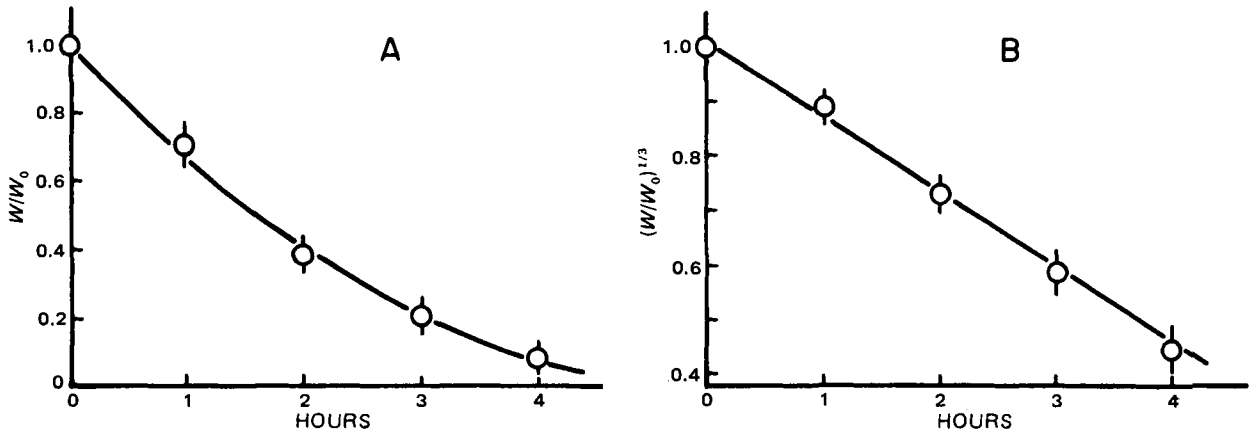

Figure 1—*Time course of* p-*hydroxyazobenzene absorption from subcutaneous injection site. Each point represents the mean of at least four experiments; vertical bar shows the standard deviation.* C_0 = *1 mg/ml;* V_0 = *0.5 ml.*

were studied (2). It was concluded that the absorption from this system was solution rate limited. Visual observations of present experimental systems supported this conclusion, since the tissue fluid colored by the dissolution of a dye was almost limited to the narrow region close to the surface of the particles or their agglomerate except for a short period immediately after injection.

On the basis of the above findings, it is assumed that the absorption is controlled by diffusion from the surface of the agglomerate. The process of this absorption seems to have a resemblance to that observed after intramuscular injection. Thus, the absorption model proposed for the intramuscular injection in a previous study (4) is expected to be applicable to the subcutaneous injection as well. From that model the following kinetic equations could be derived to describe the intramuscular absorption process (4). The fraction of the drug amount (W) remaining at the injection site to the dose (W_0) was given as a function of time (t):

$$(W/W_0)^{1/3} = 1 - jt \qquad \text{(Eq. 1)}$$

where j was defined as an absorption rate constant. This j could be related to the *in vivo* solubility (C_s), density of the drug crystal (ρ), *in vivo* dissolution rate constant (k), and the dose (W_0), using a correction parameter (ϵ) for the effective surface area of the particle agglomerate for the *in vivo* dissolution:

$$j = k\epsilon C_s \rho^{-2/3} W_0^{-1/3}/3 \qquad \text{(Eq. 2)}$$

In this equation the parameter ϵ was assumed to be an unknown function of the effective particle size (D), initial volume concentration (C_0/ρ) of the suspended drug, injection volume (V_0), and other factors (U) containing hydrodynamic factors (injection speed and pressure) and the histological and physiological factors in the injection site:

$$\epsilon = F(D, C_0/\rho, V_0, U) \qquad \text{(Eq. 3)}$$

The relationship between ϵ (or j) and C_0, V_0, or D was investigated experimentally (4).

In the present study, the above kinetic relationships proposed for the intramuscular absorption were checked to ascertain their applicability for the subcutaneous absorption and then developed to gain greater understanding of its phenomena.

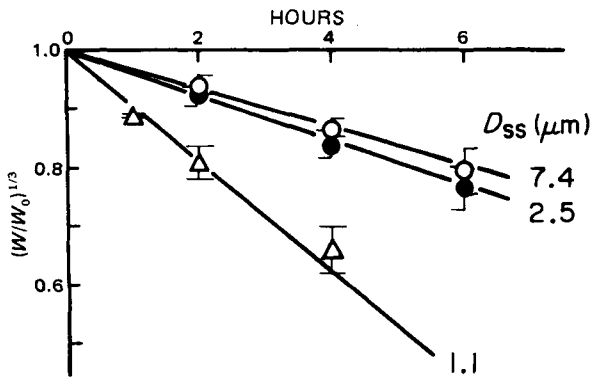

Figure 2—*Effect of particle size on subcutaneous absorption of* p-*hydroxyazobenzene. Each point represents the mean of at least three experiments; vertical bar indicates the standard deviation.* C_0 = *5 mg/ml;* V_0 = *0.5 ml.*

Time Course of Drug Absorption—First, the validity of Eq. 1 was checked experimentally. Figure 1 shows a plot of the residual fraction (W/W_0) or its cube root of the drug remaining in the injection site against time after dorsal subcutaneous administration of the controlled aqueous suspension of *p*-hydroxyazobenzene into intact rats. The initial drug concentration (C_0) and injection volume (V_0) are given in the legend. The cube root plot (B) gave a good linear relationship while the other (A) showed an upward curvature. This tendency was common throughout the following absorption experiments of different conditions, and the correlation coefficient obtained by the least-squares linear regression from the cube root plot was always larger than that from the linear plot. These results suggest that Eq. 1 is appropriate for describing the time course of the subcutaneous drug absorption from aqueous suspensions. In addition, the moderate magnitude of the standard deviations shown in Fig. 1 demonstrated that the other factors (U) in the parameter ϵ might be well-controlled under the experimental conditions in this study.

Effect of Particle Size on Absorption—The particle size of a suspension is an important factor for intramuscular (12–14) and subcutaneous absorption (1) as well as for absorptions from other routes (15). If the suspension particles are dispersed at the injection site too extensively to aggregate with each other, and, hence, the drug transport from the surface of each particle takes place independently, the particle size effect on the absorption may appear most strongly. In such a case, theoretically, $\epsilon = 6(W_0/\rho)^{1/3}/D$ for monodispersed spherical particles (diameter, D) and therefore is inversely proportional to the particle size (4). However, this is expected to be rare in practice because of the agglomerate formation in the injection site, except in an exceedingly dilute suspension with very fine particles. Thus, the relationship between the drug absorption

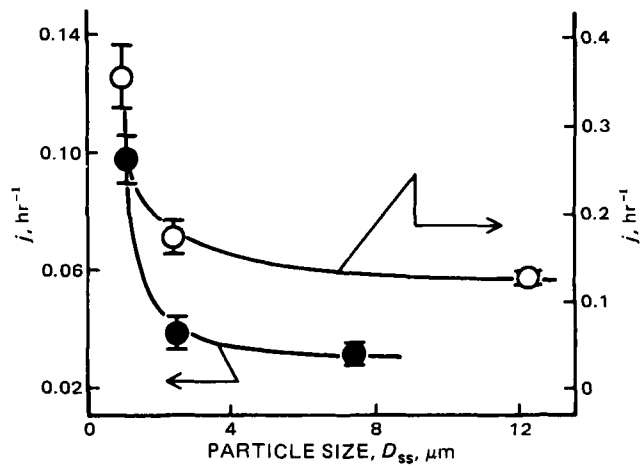

Figure 3—*Relation between absorption rate constant* (j) *and particle size* (D_{ss}). *The value of* j *was estimated by the least-squares method and is plotted with the standard error. Key:* —●—, *sc* (V_0 = *0.5 ml*); —○—, *im* (V_0 = *0.05 ml*); p-*hydroxyazobenzene concentration of both injections, 5 mg/ml.*

Table IV—Comparison of Subcutaneous Absorption Rate Constants (j) with *In Vitro* Solubilities (C_s' and C_s'') and Values of $MW^{-0.5}\rho^{-0.34}$

Compound	*In Vitro* Solubility C_s', mg/ml[a]	*In Vitro* Solubility C_s'', mg/ml[b]	$MW^{-0.5}\rho^{-0.34}$ [c]	j, hr^{-1} [d]
Sulfamethoxazole	5.7[e]	7.2	0.0549	0.374 (0.015)
N^1-Acetylsulfamethoxazole	0.076	<0.76	0.0522	0.168 (0.013)
p-Aminoazobenzene	0.049	0.41	0.0672	0.0652 (0.0037)
p-Hydroxyazobenzene	0.034	<0.69	0.0637	0.0420 (0.0035)
o-Aminoazotoluene	0.007	<0.14	0.0625	0.0193 (0.0016)
1-Phenylazo-2-naphthylamine	0.0003	0.076	0.0585	0.00241 (0.00014)

[a] Solubility in saline [0.9% (w/v) NaCl aqueous solution] at 37°. [b] Solubility in 2% (w/v) bovine serum albumin in pH 7.25 isotonic phosphate buffer at 37°. [c] MW, molecular weight; ρ, density. This term is defined in detail in the text. [d] Value estimated by the least-squares method from the data shown in Fig. 6; listed with the standard error in parentheses. [e] Solubility in pH 7.25 isotonic phosphate buffer at 37° (solubility in saline at 37°, 0.61 mg/ml). Solubilities of other test compounds in saline agreed well with those in the buffer.

rate and particle size seems to be very complicated. A previous study on the intramuscular absorption showed that the increase in the absorption rate constant (j) with decreasing mean particle diameter (D_{ss}) was remarkable in the region of D_{ss} smaller than 2–3 μm, while it was gradual or slight in the region above this (4).

Figure 2 compares subcutaneous absorption time profiles of *p*-hydroxyazobenzene from three preparations with different mean particle diameters (D_{ss}) but with similar distribution constants (n) and sedimentation volumes (V_{sed}): D_{ss} (n), 7.4 μm (2.5), 2.5 μm (2.8), and 1.1 μm (2.9); V_{sed}, 2.8–3.2 cm^3/g. The absorption rate constant (j) was obtained from the slope of each linear relationship in this figure and then plotted against D_{ss} in Fig. 3. For comparison, the results from similar experiments of the intramuscular route (m. gastrocnemius) are also shown. Figure 3 suggests that the relationship between j and D_{ss} for the subcutaneous route is qualitatively similar to that for the intramuscular route. The particles smaller than 2–3 μm in diameter seem to pass more easily through the network of the fibrous tissues accompanying the spreading of the dispersion medium during injection. This may cause a looser agglomeration of the particles and result in the abrupt change in j below this particle size.

Figure 4 shows the effect of particle size on the lateral spreading of the particle agglomerate. Here, six water-insoluble standard particles with different mean diameters ($\bar{D}$, obtained from the number size distribution curve) were used for comparison. The similarity of the form of this curve to those in Fig. 3 may support the above speculation. The participation of direct absorption mechanisms involving phagocytosis must be also considered but their contributions seem to be relatively small under the present experimental conditions. In any event, the tendency of the particle size effect appears to have a very important practical meaning.

Effect of Initial Drug Concentration and Injection Volume—If the injected particles form no agglomerate and the drug transport from each particle proceeds independently, and if this process is a rate-determining step, the absorption rate constant (j) does not depend on the dose and is inversely proportional to the particle size as mentioned previously. However, this was not the case for the subcutaneous injection of ordinary aqueous suspensions. The absorption rate constant (j), given by Eq. 2, is a function of the dose W_0 and the parameter ϵ. The term W_0 is the product of the initial drug concentration (C_0) and injection volume (V_0). The parameter ϵ is assumed to depend on C_0 and V_0, but their relationship is not known. Therefore, the quantitative relationship between j and C_0 or V_0 is also not clear.

To elucidate this relationship, the absorption time courses of the controlled suspensions of *p*-hydroxyazobenzene with different C_0 and V_0 were followed, then their absorption rate constants (j) were obtained from the same plot as Fig. 1B. In Fig. 5 j is plotted against C_0 at fixed V_0 (0.5 ml) or against V_0 at fixed C_0 (5 mg/ml) on a log–log scale. The linear relationships of both plots allow the following tentative and approximate representation:

$$j = fC_0^g V_0^h \qquad \text{(Eq. 4)}$$

where f is a constant that depends on the drug and its suspension preparation.

Thus, the experimental values of g and h were estimated by multiple regression analysis from 12 sets of data for the controlled suspensions of *p*-hydroxyazobenzene. The original data used for this estimation and resulting g and h values are summarized in Table II. Next, to ascertain the applicability of these experimental values ($g = -0.66$ and $h = -0.32$), additional examinations were done using aqueous suspensions of betamethasone dipropionate. Employing Eq. 4 and the g and h values determined above, the ratio of $j(i)$ at $C_0(i)$ and $V_0(i)$ to $j(1)$ at $C_0(1)$ and $V_0(1)$ for suspensions with the same drug and similar colloidal properties can be represented as:

$$j(i)/j(1) = [C_0(i)/C_0(1)]^{-0.66}\,[V_0(i)/V_0(1)]^{-0.32} \qquad \text{(Eq. 5)}$$

Table III compares the calculated and experimental ratios $j(i)/j(1)$ for the case where $C_0(i)/C_0(1) = 10$ or $V_0(i)/V_0(1) = 10$. These comparisons showed good mutual agreements, despite the fact that the vehicle and the colloidal properties of the suspensions tested here differed considerably from those of the controlled suspension of *p*-hydroxyazobenzene used for the estimation of g and h values. Therefore, Eq. 5, obtained ex-

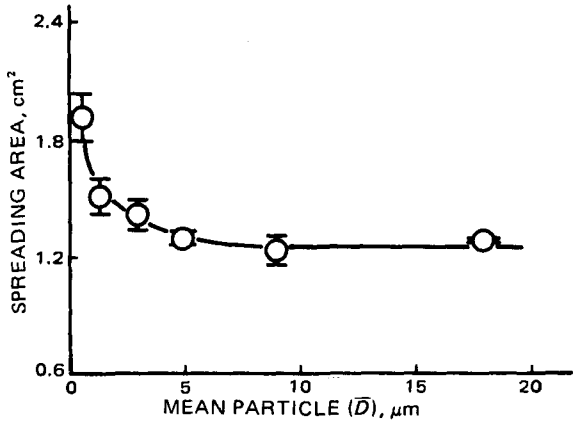

Figure 4—*Effect of particle size on the lateral spreading area of the particle agglomerate formed by subcutaneous injection of aqueous suspension. Each point represents the mean of three experiments; vertical bar indicates the standard deviation. These data were obtained using water-insoluble standard particles of various sizes under the following conditions:* C_0 *= 5 mg/ml;* V_0 *= 1.0 ml; measurement, 5 min after injection.*

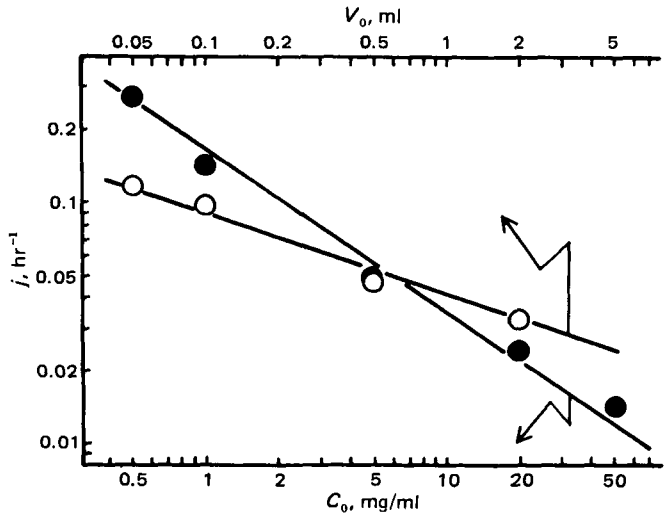

Figure 5—*Relation between absorption rate constant* (j) *and injection volume* (V_0) *or initial drug concentration* (C_0) *for the controlled suspension of* p*-hydroxyazobenzene. The value of* j *was estimated by the least-squares method. Key: —●—, constant* V_0 *(0.5 ml); —○—, constant* C_0 *(5 mg/ml).*

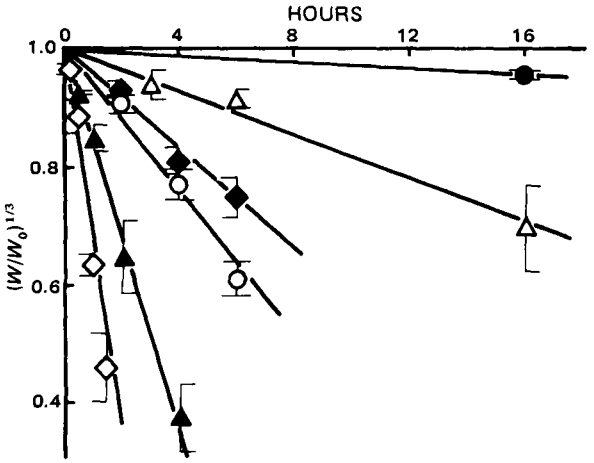

Figure 6—*Comparison of absorption rate among various compounds (controlled suspension). Each point represents the mean of three or four experiments; vertical bar indicates the standard deviation.* C_0 *= 5 mg/ml;* V_0 *= 0.5 ml. Key: —●—, 1-phenylazo-2-naphthylamine; —△—, o-aminoazotoluene; —◆—, p-hydroxyazobenzene; —○—, p-aminoazobenzene; —▲—,* N^1*-acetylsulfamethoxazole; —◇—, sulfamethoxazole.*

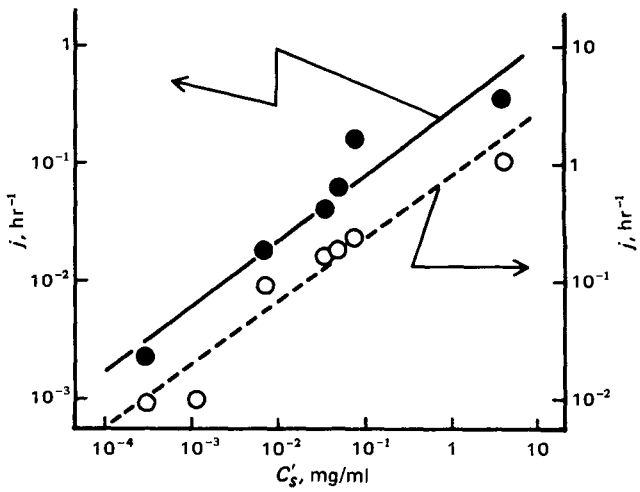

Figure 7—*Relationship between absorption rate constant* (j) *and in vitro solubility* (C_s'). *The value of* j *was estimated by the least-squares method from the data shown in Fig. 6. Key: —●—, sc* (C_0 *= 5 mg/ml;* V_0 *= 0.5 ml); —○—, im* (C_0 *= 5 mg/ml;* V_0 *= 0.05 ml), cited from a previous study (4).*

perimentally, is expected to be generally applicable for aqueous suspensions other than the model ones tested here.

Using the above results, the relationship between the parameter ϵ and C_0 or V_0 can be clarified empirically in the following manner:

$$j = fC_0^{-0.66}V_0^{-0.32} \quad \text{(Eq. 6)}$$

Employing the relationship $W_0 = C_0V_0$, Eq. 2 can be rewritten as:

$$j = kC_s\rho^{-2/3}\epsilon C_0^{-1/3}V_0^{-1/3}/3 \quad \text{(Eq. 7)}$$

From the equivalency of Eqs. 6 and 7, the parameter ϵ must satisfy the following relationship:

$$\epsilon = F(D, C_0/\rho, V_0, U) = \delta(C_0/\rho)^{-0.33}V_0^{0.01} \quad \text{(Eq. 8)}$$

where δ is a term that depends on the remaining factors D and U. Equation 8 means that the parameter ϵ depends little on the injection volume (V_0) but decreases by increasing initial drug concentration (C_0). This also implies that the degree of agglomeration may tend to increase with an increase in C_0. Substitution of Eq. 8 for ϵ in Eq. 7 yields:

$$j = (kC_s\delta/3)\rho^{-0.34}C_0^{-0.66}V_0^{-0.32} \quad \text{(Eq. 9)}$$

The above empirical equation obtained for the subcutaneous route demonstrates a great similarity to that for the intramuscular route, which was given by the following equation (4):

$$j_m = (k_mC_s\delta_m/3)\rho^{-0.45}C_0^{-0.55}V_0^{-0.32} \quad \text{(Eq. 10)}$$

It should be noted that the correlation between the absorption rate constant and injection volume is identical for the two routes.

Although Eqs. 9 and 10 are derived empirically, they should be very important and useful since they give relationships between the dose and absorption rate constant which have been unknown until now.

Comparison of Absorption Rate among Various Compounds—Equation 9 shows that the absorption rate constants (j) of different compounds depend upon the values of k, C_s, and ρ when the preparation-dependent parameters (δ) are the same. As defined previously, ρ, k, and C_s represent the density of the drug, the *in vivo* dissolution rate constant, and *in vivo* solubility in the injection site, respectively. Of these factors, only the value of ρ can be determined by an *in vitro* experiment; the other two (k and C_s) cannot be completely estimated from such an experiment. From a practical point of view, an attempt was made to clarify the quantitative relationship between j and the above three factors (or their first approximations).

Figure 6 compares the subcutaneous absorption time profiles of six test compounds. In this comparison, the controlled suspensions with similar colloidal properties (Table I) were used to minimize the variation in δ in Eq. 9. All the compounds gave good linear relationships with different slopes. Their observed absorption rate constants (j) are summarized in Table IV with their physicochemical factors such as *in vitro* solubilities in saline and 2% (w/v) bovine serum albumin (C_s' and C_s'', respectively).

As discussed previously, the absorption is inferred to be a diffusion-controlled process. Diffusion coefficients of compounds having low molecular weight (MW) are known to be inversely proportional to the square root of MW (16). The *in vivo* dissolution rate constant (k) in Eq. 9 is considered to be proportional to the diffusion coefficient, like that *in vitro* (2, 17). Therefore, Eq. 9 can be converted to

$$j = (\theta\delta/3)\mathrm{MW}^{-0.5}\rho^{-0.34}C_sC_0^{-0.66}V_0^{-0.32} \quad \text{(Eq. 11)}$$

where θ is a constant. Thus, the values of $\mathrm{MW}^{-0.5}\rho^{-0.34}$ for model drugs were calculated and are in Table IV as the correction term. However, these values were similar to each other for the compounds tested here. In contrast, the *in vitro* solubility was a more dominant factor and had a positive relation with the absorption rate constant.

Equation 11 means that the plot of j (or $j_{corr} = j\mathrm{MW}^{0.5}\rho^{0.34}$, if the correction for MW and ρ is necessary) against *in vivo* solubility (C_s) on a log–log scale gives a straight line with a slope of unity at the constant initial drug concentration (C_0) and injection volume (V_0). The closed circles in Fig. 7 show this plot using *in vitro* solubility (C_s') in Table IV instead of *in vivo* solubility (C_s). This gave a nearly straight line with a slope of 0.53 (regression equation, $\log j = 0.525 \log C_s' - 0.578$; correlation coefficient, $r = 0.956$). Using j_{corr} in place of j, a similar relationship was also obtained ($\log j_{corr} = 0.534 \log C_s' + 0.660$, $r = 0.953$).

In Fig. 7, similar data for the intramuscular administration (m. gastrocnemius), cited from a previous study (4), are also plotted with open circles. Remarkably, the slopes of these plots for the two routes were almost identical. This shows a strong similarity in the absorption mechanism between the two routes. The deviation of the slope from unity observed in Fig. 7 may be attributed mainly to a gradual increase in the ratio C_s/C_s' with decreasing C_s' caused by the relatively larger solubilization effect of the protein components in the body fluid for the drug having a smaller solubility. The comparison of C_s' and C_s'' in Table IV supports this explanation.

The good linear relationship between $\log j$ (or $\log j_{corr}$) and $\log C_s'$ mentioned previously is expected to be applicable for predicting the subcutaneous absorption rates of other compounds in the controlled suspensions from C_s'. For instance, the prediction (from the regression equation, $\log j_{corr} = 0.534 \log C_s' + 0.660$) for the test material, betamethasone dipropionate (MW = 504; $\rho = 1.23$ g/cm^3; $C_s' = 0.002$ mg/ml) gave a value of 0.007 hr^{-1} for j (at $C_0 = 5$ mg/ml and $V_0 = 0.5$ ml), which almost agreed with the experimental value of 0.0096 ($\pm$0.0011) hr^{-1} observed using the following controlled suspension: $D_{ss} = 4.3$ μm; $n = 2.6$. This satisfactory result suggests that similar prediction will be possible for other drugs.

Comparison of Absorption Rates between Subcutaneous and Intramuscular Routes—Hitherto, drug absorption kinetics and mechanisms from aqueous suspensions in the subcutaneous route have been clarified, and their strong similarity to those by the intramuscular route, discussed previously (4), have been pointed out. A direct comparison of absorption rates between the two routes seems to be usable but there has been little available data (18). Table V shows this com-

Table V—Comparison of Absorption Rate Constants (j) between Subcutaneous (sc) and Intramuscular (im) Routes [a]

Compound	j, hr^{-1}	
	sc[b]	im[c]
Sulfamethoxazole	0.78	1.10 ± 0.07
p-Aminoazobenzene	0.14	0.18 ± 0.01
p-Hydroxyazobenzene	0.090 (0.12 ± 0.02)[d]	0.17 ± 0.01
o-Aminoazotoluene	0.040	0.093 ± 0.005
1-Phenylazo-2-naphthylamine	0.0050	0.0093 ± 0.0006

[a] Controlled suspension. C_0, 5 mg/ml; V_0, 0.05 ml. [b] Estimated by extrapolation of data shown in Table IV using Eq. 5. [c] Experimental data (with standard error) cited from the previous report (4). [d] Experimental value (with standard error).

parison using five controlled suspensions. To compare at the same drug concentration (C_0) and injection volume (V_0), the values estimated by extrapolation of the data shown in Table IV using Eq. 5 were used for the absorption rate constants (j) in the subcutaneous route. This comparison shows that the absorption rate from the subcutaneous route is slower than that from the intramuscular route for all the test suspensions. A similar tendency was previously observed for injections of drug-oil solutions (5). The relationship between j and C_0 in the subcutaneous route differed slightly from that in the intramuscular route (Eqs. 9 and 10). Therefore, it should be noted that the difference in j shown in Table V may increase with increasing C_0.

REFERENCES

(1) V. G. Foglia, J. C. Penhos, and E. Montuori, *Endocrinology*, **57**, 559 (1955).

(2) B. E. Ballard and E. Nelson, *J. Pharmacol. Exp. Ther.*, **135**, 120 (1962).

(3) B. E. Ballard and E. Nelson, *J. Pharm. Sci.*, **51**, 915 (1962).

(4) K. Hirano, T. Ichihashi, and H. Yamada, *Chem. Pharm. Bull.*, **29**, 817 (1981).

(5) K. Hirano, T. Ichihashi, and H. Yamada, *J. Pharm. Sci.*, **71**, 495 (1982).

(6) E. A. Brown, T. G. Metcalf, and L. W. Slanetz, *Ann. Allergy*, **19**, 1016 (1961).

(7) F. L. Ashley, S. Braley, T. D. Rees, D. Goulian, and D. L. Ballantyne, Jr., *Plastic Reconstruc. Surg.*, **39**, 411 (1967).

(8) C. R. Beresford, L. Golberg, and J. P. Smith, *Br. J. Pharmacol.*, **12**, 107 (1957).

(9) T. D. Rees, D. L. Ballantyne, Jr., I. Seidman, and G. A. Hawthorne, *Plastic Reconstruc. Surg.*, **39**, 402 (1967).

(10) J. Lewin and F. Huidobro, *Acta Physiol. Lat. Am.*, **3**, 17 (1953).

(11) E. Secher-Hansen, H. L. Langgard, and J. Schou, *Acta Pharmacol. Toxicol.*, **26**, 9 (1968).

(12) F. H. Buckwalter and H. L. Dickison, *J. Am. Pharm. Assoc. Sci. Ed.*, **47**, 661 (1958).

(13) L. G. Miller and J. H. Fincher, *J. Pharm. Sci.*, **60**, 1733 (1971).

(14) N. Kitamori, S. Kawaziri, and T. Matsuzawa, "Abstracts of Papers," 93th Annual Meeting of Japan Pharmaceutical Society, Tokyo, April 1973, p. 266.

(15) J. H. Fincher, *J. Pharm. Sci.*, **57**, 1825 (1968).

(16) W. D. Stein, "The Movement of Molecules across Cell Membranes," Academic, New York, N.Y. 1967, p. 67.

(17) W. Nernst, *Z. Phys. Chem.*, **47**, 52 (1904).

(18) J. J. Nora, W. D. Smith, and J. R. Cameron, *J. Pediatr.*, **64**, 547 (1964).

ACKNOWLEDGMENTS

The authors thank Mrs. J. Kagawa for her technical assistance and Prof. M. Nakagaki, Kyoto University, for his valuable comments on the manuscript.

Dissolution and Bioavailability Studies of Whole and Halved Sustained-Release Theophylline Tablets

KEITH J. SIMONS **, EVELYN M. FRITH ‡, and F. ESTELLE R. SIMONS ‡

Received July 24, 1980, from the **Faculty of Pharmacy, and* ‡ *Section of Allergy and Clinical Immunology, Department of Pediatrics, Faculty of Medicine, University of Manitoba, Winnipeg, Manitoba, Canada, R3T 2N2.* Accepted for publication August 5, 1981.

Abstract □ In dissolution studies of whole and halved 100-mg sustained-release theophylline tablets, drug release from halved tablets was significantly higher. These differences were not reflected in the bioavailability studies. The area under the curve (AUC) mean absorption time and fraction-of-dose recovered in urine at 24 hr were not significantly different following the ingestion of whole or halved 100-mg tablets. The elimination rate constant, half-life, volume of distribution, plasma, and renal clearance values were consistent with values reported previously. Discrepancies were found in the 24-hr metabolite distribution as compared to literature values and may be accounted for by the age and health of the subjects and the frequency of dosing.

Keyphrases □ Dissolution—whole and halved sustained-release theophylline tablets □ Sustained-release system—dissolution of whole and halved theophylline tablets □ Bioavailability—whole and halved sustained-release theophylline tablets □ Theophylline—bioavailability and dissolution study of whole and halved sustained-release tablets

Breaking sustained-release theophylline tablets in half is commonly practiced to achieve more accurate milligrams per kilogram dosing in children. The extent to which this affects dissolution and bioavailability is unknown.

In this investigation, 100-mg sustained-release theophylline tablets[1] were used to study the effect of halving tablets on dissolution and bioavailability. No published information about the dissolution of these tablets was available. After oral administration of the 100-mg tablet, however, 90% of the dose was absorbed within 14 hr and almost 100% was absorbed by 28 hr (1). When 300-mg tablets were dissolved, 50% of the dose entered solution by 2 hr and > 90% of the dose entered solution by 6 hr (1).

EXPERIMENTAL

Dissolution—The official USP dissolution apparatus was used (2). Simulated gastric and intestinal fluids were used as dissolution media (2).

Simulated gastric fluid, USP (2), was prepared by dissolving 2 g of sodium chloride and 3.2 g of pepsin in 7 ml of HCl and diluting the solution to 1000 ml with distilled water. This test solution had a pH of 1.2.

Simulated intestinal fluid, USP (2), was prepared by dissolving 6.8 g

[1] Theo-Dur, Astra Pharmaceuticals Canada Ltd., Mississauga, Canada L4X 1M4.

0022-3549/82/0500-0505$01.00/0